Mixed hemi/ad-micelle sodium dodecyl sulfate-coated magnetic iron oxide nanoparticles for the efficient removal and trace determination of rhodamine-B and rhodamine-6G

Mixed hemi/ad-micelle SDS-coated magnetic iron oxide nanoparticles for the efficient removal and trace determination of rhodamine-B and rhodamine-6G

Elias Ranjbari[†,‡], Mohammad Reza Hadjmohammadi[‡,*], Filip Kiekens[§], and Karolien De Wael[‡]

[†]AXES, Department of Chemistry, University of Antwerp, Groenenborgerlaan 171, 2020 Antwerp, Belgium, [‡]Department of Analytical Chemistry, Faculty of Chemistry, University of Mazandaran, Babolsar, Iran, and [§]Department Pharmaceutics, Campus Drie Eiken, University of Antwerp, Antwerp, Belgium

Corresponding Author's Tel & fax: +981135302391; E-mail address: hadjmr@umz.ac.ir

ABSTRACT: Mixed hemi/ad-micelle SDS-coated magnetic iron oxide nanoparticles (MHAMS-MIONPs) were used as an efficient adsorbent for both removal and preconcentration of two important carcinogenic xanthine dyes named rhodamine-B (RB) and rhodamine-6G (RG). To gain insight in the configuration of SDS molecules on the surface of MIONPs, zeta potential measurements were performed in different [SDS]/[MIONP] ratios. Zeta potential data indicated that mixed hemi/ad-micelle MHAM was formed in [SDS]/[MIONP] ratios over the range of 1.1 to 7.3. Parameters affecting the adsorption of dyes were optimized as removal efficiency by one variable at-a-time and response surface methodology; the obtained removal efficiencies were ~100%. Adsorption kinetic and equilibrium studies, under the optimum condition (pH = 2; amount of MIONPs = 87.15 mg; [SDS]/[MIONP] ratio = 2.9), showed that adsorption of both dyes are based on the pseudo-second-order and the Langmuir isotherm models, respectively. The maximum adsorption capacities for RB and RG were 385 and 323 mg g^{-1}, respectively. MHAMS-MIONPs were also applied for extraction of RB and RG. Under optimum condition (pH = 2; amount of damped MHAMS-MIONPs = 90 mg; eluent solvent volume = 2.6 mL of 3% acetic acid in acetonitrile), extraction recoveries for 0.5 mg L^{-1} of RB and RG were 98% and 99%, with preconcentration factors of 327 and 330, respectively. Limit of detection obtained for rhodamine dyes were <0.7 ng mL^{-1}. Finally, MHAMS-MIONPs were successfully applied for both removal and trace determination of RB and RG in environmental and waste water samples.

INTRODUCTION

Rhodamine-B (RB) and rhodamine-6G (RG) with multi-ring aromatic xanthene core planar structure are two of the most popular fluorescent synthetic dyestuffs.[1] RB and RG were used initially as colorant in textile and food industry, and later they found wide usage as water tracer, petroleum products dyeing, paper printing, forensic technology, color photography and cosmetic products. Although the toxicity, mutagenicity, and carcinogenic activities of RG and RB have been experimentally proven,[2-5] nonetheless these harmful dyes are still illicitly used in some parts of the world, due to their low cost and high efficacy.[6]

Owing to high solubility in water, RB and RG are easily released into the environment, especially into the water resources, during the process of production, manufacture, usage and disposal of the goods containing these dyes. Releasing these pollutants into the environment, will lead to serious consequences on the health of human beings, plants, animals, and microbes; therefore, making efforts to develop a procedure for removal of these carcinogenic dyes from waste waters, and environmental waters is necessary. Also, providing a sensitive and reliable method for determination of trace amounts of RB and RG for quality control of water samples is inescapable.

Several approaches have been reported in the literature dealing with the removal of rhodamine dyes from aqueous samples either by destruction of the dye molecular structure through photocatalytic degradation,[7] ultrasonic degradation,[8] and sonochemical degradation,[9] or by adsorption of the rhodamine molecules at the surface of the adsorbents such as sodium montmorillonite,[10] palm shell-based activated carbon,[11] and walnut shell charcoal.[12] Magnetic nanoparticle-based adsorbents are efficient adsorbents due to their unique advantages over traditional ones; they not only possess high surface area which can exhibit higher adsorption capacity for analytes, but also they have strong magnetic properties which can provide the isolation of sorbents from sample solutions by the application of an external magnetic field; thus, no centrifugation of the sample is needed after treatment (in comparison with non-magnetic adsorbents).[13-15]

Up to now, analysis of RB and RG has been done by various instrumental techniques, such as UV-Vis[16,17] and fluores-

cence[18] spectrophotometry, high-performance liquid chromatography (HPLC) coupled with UV-Vis detection[19] and fluorescence detection[20] as well as ultra-performance liquid chromatography tandem mass-spectrometry.[21] However, due to the very low concentration levels of RG and RB in environmental water samples and the complexity of the different matrices, the direct use of spectrometric and chromatographic methods are limited by their selectivity and sensitivity, and that is why the sample preparation and preconcentration of analytes are momentous steps in analytical methods prior to instrumental analysis.

Despite the widespread usage of RB and RG in several industries, only few literature were paid attention to the sample preparation and preconcentration of these carcinogenic compounds aimed to simultaneous determination of them.[19,20,22] In previous work,[19] we applied magnetic stirring assisted dispersive liquid-liquid microextraction (MSA-DLLME), based on extraction solvent with lower density than water, while Xiao et al.[22] determined these dyes by dispersive liquid-liquid microextraction method based on extraction solvent with higher density than water. Chiang et al.[20] applied solid phase extraction (SPE) method based on HLB-cartridge for the extraction of these two synthetic dyes from surface water and municipal wastewater samples. In recent years, nanoparticles, particularly magnetic nanoparticles (MNPs), have been emerging as a new type of important functional solid phase extraction material. Magnetic nanoparticle-based solid phase extraction (MNP-SPE) consists of two main steps: firstly, in adsorption step, analytes are adsorbed on the surface of MNPs and in the second step, the adsorbed analytes will be desorbed from the surface of MNPs in a suitable solvent for the analysis by an appropriate analytical instrument.

The aim of the ongoing study is utilization of magnetic iron oxide nanoparticles (MIONPs) for both removal and trace determination of RB and RG dyes in waste water and environmental water samples. Despite the advantages of MIONPs, they are very sensitive dealing with oxidation and agglomeration; therefore, several organic[23-25] and inorganic[26-28] coatings were applied until now, which winamp protection of MIONPs, they provide a competent substrate at the surface of the particles for adsorption of analytes. Surface modification of synthesized MIONPs was done by self-assembly of sodium dodecyl sulfate (SDS) as mixed hemi/ad-micelle (MHAM) around MIONPs. To the best of our knowledge, this is the first report of zeta potential studies to gain insight in the configuration of SDS molecules on the surface of MIONPs; although, some literature reported zeta potential data for SDS coating of alumina[29] and magnetic graphene sheets,[30] previously. The parameters affecting the adsorption of RB and RG by mixed hemi/ad-micelle SDS coated magnetic iron oxide nanoparticles (MHAMS-MIONPs) were optimized and the best condition was applied to remove the rhodamine dyes from the waste and environmental water samples. Finally, MHAMS-MIONPs were used for MNP-SPE of trace amounts of RB and RG, and after optimization of parameters affecting on extraction, the procedure was successfully applied for the analysis of different water samples.

EXPERIMENTAL SECTION

Chemicals. Standards of RB (≥97%) and RG (99%), methanol (HPLC-grade), ethanol (HPLC-grade), acetone (HPLC-grade), acetonitrile (HPLC-grade), were purchased from Sigma. The water used for the mobile phase was milli-Q water. Individual stock solutions of each dyes compound were prepared in methanol and a standard mixture solution of all target compounds was prepared in methanol at a final concentration of 1000 mg L^{-1}. The working solution was prepared by appropriate dilution of the stock solution with distilled water. All of the standard solutions were stored at 4 ° C and brought to ambient temperature just prior to use. The instrumentation and operating conditions were described in Supporting Information (SI).

Preparation of SDS-coated MIONPs. MIONPs were synthesized by a published co-precipitation method based on formation of iron oxides from aqueous Fe^{2+}/Fe^{3+} salt solutions in the presence of a base;[31] the details of synthesis steps was described in Supporting Information (SI), as well as characterization of the synthesized MIONPs (Figure S-1). The synthesized MIONPs, which have a large ratio of surface area to volume, tend to agglomerate in order to reduce their surface energy.[32] Modification of the NPs surface is a suitable way to prevent this phenomenon.[33, 34] In general, surface modification can be accomplished by physical or chemical adsorption of the desired molecules to coat the surface, depending on the specific applications. After synthesis of MIONPs, hydroxyl groups around nanoparticles leads to an isoelectric point at pH 6.5.[35] Regarding to the utilization of SDS (an anionic surfactant) for modification of MIONPs and respect to the isoelectric point of MIONPs, the modification was performed at pH 5. Then, using a shaker, they were mixed for 3 min to form the suspension of SDS-coated MIONPs. Depending on the amount of surfactant added to MIONPs, three different kinds of SDS-coated MIONPs, including hemi-micelle, ad-micelle and mixed hemi/ad-micelle (MHAM), can be prepared. The main advantage of MHAM array above the two other arrays is the ability of MHAM in establishing of both columbic and hydrophobic interactions with cationic form of RB and RG dyes. In order to achieve MHAMS-MIONPs, the desired ratios of SDS concentration to the MIONP concentration ([SDS]/[MIONP]) were obtained by zeta potential studies.

Experiments for optimization of dye adsorption on the surface of MHAMS-MIONPs. The adsorption step, which is enforceable for the removing goals from the environmental waters, waste waters or factories effluents, is called removal step. Various parameters affecting on the removal of the dye were studied and optimized. Investigation of the pH factor was performed by one variable at a time; and because of the significant interaction, the two other significant factors, i.e. amount of MIONPs and [SDS]/ [MIONP] ratio, were optimized by response surface methodology through central composite design (CCD). Optimization studies were carried out according to the following procedure: (1) pH of 50 mL aqueous solution of the dyes (50 mg L^{-1}) was adjusted to desired value; (2) pH of the MIONP suspension (with certain amount of MIONPs) was adjusted in 5; (3) then a specified amount of SDS was added into the MIONP suspension and using a shaker they were mixed for 3 min to form the suspension of SDS-coated MIONPs; (4) the SDS-coated MIONPs were separated from the water and free SDS molecules using a super magnet

(1.3 T), and the aqueous phase was poured out; (5) aqueous solution of sample, from step (1), was added to the SDS-coated MIONP and the suspension was stirred for 5 minutes; after dye adsorption; (6) MIONPs were separated from the sample solutions using the magnet; and (7) the residual dyes concentrations in the supernatant solution were determined by HPLC-Vis using a calibration curve. To compare the different conditions of removal, the removal efficiency (*RE*%) was applied which can be obtained by the following equation:

$$RE\% = \frac{C_0 - C_r}{C_0} \times 100 \quad (1)$$

where C_0 and C_r are the initial and residual concentrations of the dye in the solution (mg L^{-1}), respectively.

Experiments for optimization of dye desorption from the surface of MHAMS-MIONPs. Desorption studies were performed not only to recover the dyes from the adsorbent, but also they were carried out to restore the adsorption capacity of the exhausted adsorbent and to reuse the MIONPs. Furthermore, desorption process after adsorption is very important for MNP-SPE of trace amounts of dyes in the water samples. In MNP-SPE of RB and RG, the dyes previously adsorbed on the surface of MHAMS-MIONPs were desorbed by a suitable elution solvent. Then the eluent was completely separated from the adsorbent, using the super-magnet, and it was evaporated to dryness under a gentle stream of nitrogen. The residue was dissolved in 150 µL of water, as injection solvent, and injected into the HPLC using a 10 µL sample loop. In order to investigate the influence of various experimental parameters on the desorption efficiency of RB and RG from the surface of MHAMS-MIONPs, we used extraction recovery % (*ER*%). The *ER*% was defined as the percentage of the total analyte (n_0) extracted into the injection solvent (n_{inj}); According to equation (2):

$$ER\% = \frac{n_{inj}}{n_0} \times 100 = \frac{C_{inj} \times V_{inj}}{C_0 \times V_0} \times 100 \quad (2)$$

where C_{inj} and C_0 are the concentrations of dyes in injection phase and initial concentration of dyes in aqueous sample, respectively. C_{inj} is determined from a calibration curve which was obtained using direct injection of standard solutions to the HPLC-Vis system. V_{inj} and V_0 are the volumes of injection phase and aqueous sample, respectively.

The preconcentration factor (*PF*) was defined as the ratio between the analyte concentration in the injection phase (C_{inj}) and the initial concentration of analyte (C_0) in the aqueous sample, as follows:

$$PF = \frac{C_{inj}}{C_0} \quad (3)$$

Combination of equations (2) and (3) gives:

$$ER\% = PF \times \frac{V_{inj}}{V_0} \times 100 \quad (4)$$

Kinetic experiments. Kinetic studies were performed in optimum condition of removal and at preset time intervals ranged from 1 to 10 min, the samples of 0.5 mL were taken from the solution to analyze the residual rhodamine dye concentration in the solution. The collected kinetic data were analyzed using pseudo-first order (equation (5),[36] pseudo-second order (equation (6)), [37] and intra-particle diffusion (equation (7)) [38] models to find out the adsorption rate expression:

$$\log(q_e - q_t) = \log q_e - \frac{k_f}{2.303} t \quad (5)$$

$$\frac{t}{q_t} = \frac{1}{k_s q_e^2} + \frac{1}{q_e} t \quad (6)$$

$$q_t = k_i t^{0.5} \quad (7)$$

where q_t (mg g^{-1}) and q_e (mg g^{-1}), are amount of dye adsorbed at each time and equilibrium, k_f (min^{-1}), k_s (g mg^{-1} min^{-1}), and k_i (mg g^{-1} $min^{-0.5}$) are the rate constants of pseudo-first-order, pseudo-second-order and intra-particle diffusion models. To select the best model, correlation coefficients (R^2) of models, as a comparative criterion, were applied for comparison. When the R^2 value is close to 1, it means that there are more accommodating between experimental data and the model-predicted values.

Adsorption isotherm studies. The equilibrium adsorption isotherm was determined using 50 mL of the dye solutions with different initial dye concentrations, 50-2000 mg L^{-1}. The time needed to reach the equilibrium condition as determined in equilibrium studies was 4.0 min. The amount of dye adsorbed per unit mass of adsorbent, q_e (mg g^{-1}), was evaluated by the following equation:

$$q_e = \frac{(C_0 - C_e)}{W} \times V \quad (8)$$

where C_0 and C_e (mg L^{-1}) are the initial and equilibrium liquid phase concentrations of the dye in the solution, respectively. W is the weight of dried MHAMS-MIONP, 0.143 g, and V is the volume of the solution, 0.05 L. The q_e obtained by this equation was 17.46 and 17.43 mg g^{-1} for 50 ppm of RB and RG solutions, respectively, which were very close to the amounts (17.51 mg g^{-1} for both dyes) obtained by the slope of pseudo-second order kinetic model.

The obtained data were compared using three isotherm equations, namely, Langmuir (equation 9),[39] Freundlich (equation 10),[40] and Tempkin (equation 11) [41] adsorption isotherm models.

$$\frac{C_e}{q_e} = \frac{1}{K_L q_{max}} + \frac{1}{q_{max}} C_e \quad (9)$$

$$\log q_e = \log K_F + \frac{1}{n} \log C_e \quad (10)$$

$$q_e = \frac{RT}{b_T}\ln A_T + \left(\frac{RT}{b_T}\right)\ln C_e \qquad (11)$$

where q_{max} is the maximum monolayer capacity of the adsorbent (mg g^{-1}), K_L the Langmuir constant (L mg^{-1}) which is related to the adsorption energy, K_F the Freundlich constant (L g^{-1}) which is an indication of the relative adsorption capacity and n the heterogeneity factor which is related to the adsorption intensity, A_T the Tempkin isotherm equilibrium binding constant (L g^{-1}), R the universal gass constant (J mol^{-1} K^{-1}), T the temperature, b_T the Tempkin isotherm constant, and (RT/b_T) which is an indicator of the heat of sorption (J mol^{-1}).

Sample preparation. The municipal waste water sample, which was provided from the waste water treatment plant of Antwerp (Belgium), effluent of University of Antwerp (UA) and Schelde River water, were analyzed as the real water samples. All samples were collected into pre-cleaned, light-preserved glass bottles and each sample was filtered through 0.45 µm membrane filters (Millipore, Bedford, MA). The measurement of the dyes was performed by standard addition method using calibration curves of 0.001– 0.01 mg L^{-1} spiked water samples.

RESULTS AND DISCUSSION

Determining MHAM condition through zeta potential studies. Zeta potential was measured by Zetasizer (Malvern Instruments Ltd., GB) and through the analyzing different suspensions of SDS-coated MIONPs with different ratios of [SDS]/ [MIONP]. All suspensions were provided by 1.0×10^{-3} mol L^{-1} NaCl as background electrolyte solution in the absence of target compounds. Figure 1 displays the zeta potential of adsorbent surface versus the [SDS]/ [MIONP] ratio. The reported zeta potentials are the average results of five repetitive measurments and the standard deviation of measurements changed in the range of 2.6 – 4.5. The zeta potential measurement of bare MIONPs indicated the value of 41.7 mV because of the positive charge of the MIONPs in acidic conditions (pH = 5). By increasing the ratio of [SDS]/ [MIONP] up to 1.1, the surface charge of MIONPs was decreased to 0.0; it means that all the MIONPs were covered by a monolayer of SDS molecules which it is called hemi-micelle. This monolayer of SDS molecular array enables the adsorbent to make the hydrophobic interaction with adsorbate. The more concentration of SDS molecules led to the second layer around the MIONPs by hydrophobic interaction of their carbon chain and the zeta potential values changed to minus values due to the negative charge of the SDS molecules in the second adsorption layer. However, the enhancement of SDS on the surface decreases the tendency of MIONPs for adsorption of more SDS, sterically and electrostatically, so that the slope of depression would be in exponential manner; insofar as making a plateau in [SDS]/ [MIONP] ratio of about 7.0. The [SDS]/ [MIONP] value of 7.3 is the ratio that all the MIONPs were covered by bilayer of SDS molecules, which is called ad-micelle and enables the adsorbent to have only the columbic interaction with adsorbate. After this ratio the zeta potential was fixed and the concentration of the SDS was increased in aqueous solution. Between the [SDS]/ [MIONP] ratios of 1.1 and 7.3, some parts of each MIONP are coated as bilayer and the other parts remain as monolayer; this self-assembly array of SDS molecules around MIONPs is called mixed hemi/ad-micelle (MHAM).

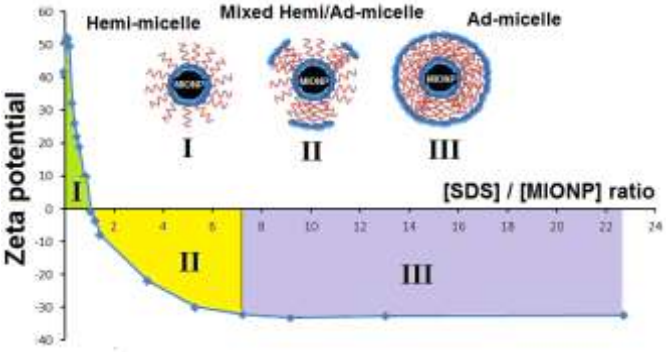

Figure 1. Zeta potential measurements in different [SDS]/ [MIONP] ratios.

The MHAM not only protects the MIONPs chemically and physically, but also this kind of SDS molecular array provides a substrate around the MIONPs, which is able to attract cationic form of RB and RG electrostatically as well as making hydrophobic interaction with them; thus, the subsequent experiments were performed using the MHAMS-MIONPs. The size distributions of MIONPs and MHAMS-MIONPs, which obtained by dynamic light scattering (DLS), as well as their transmission electron microscopy (TEM) were shown in Figure S-2 and S-3, respectively.

Effect of pH of the sample solution. pH of the solution is an important factor in protonating or deprotonating of molecules which are able to be ionized. To attract RB and RG at the negative surface of MHAMS-MIONPs, rhodamine dyes should be in their cationic form. Regarding to the acidic dissociation constant, neutral form of RG converts to its cationic form at pH 6.13 (pKa_{RG} = 6.13),[42] while transformation of RB from zwitterionic form to cationic form will take place at pH 3.2 (pKa_{RB}=3.2).[43] The experiments depicted that, by decreasing the pH of the sample, the removal efficiency will increase for both RB and RG (Figure S-4), however this enhancement is more pronounced for RB, because in pHs more than 3, zwitterion of RB can make a repulsion force to the negative charge of the surface of MHAMS-MIONPs; in the case of RG, although increasing the pH until 6 leads to the loss of positive charge and electrostatic interaction, but hydrophobic interaction prevents to the sharp decline of removal efficiency. Therefore, pH value of 2 was selected for all further experiments.

Effect of [SDS]/ [MIONP] ratio and amount of MIONP. As it was mentioned in the section 3.2., different ratios of [SDS]/ [MIONP] make different kinds of SDS coverage around the MIONPs. On the other side, the amount of MIONP determines the adsorbent dosage required for the complete removal of rhodamine dyes. In order to obtain maximum removal efficiency with the lowest amount of MIONPs, the effects of [SDS]/[MIONP] ratio and amount of MIONPs were considered, simultaneously. To evaluate the significance of each effect and to estimate the interaction of these two parameters, response surface methodology was applied using a CCD of experiments. Based on the CCD, totally 16 experiments

were carried out in a randomized manner in order to minimize the effect of uncontrollable variables (see Table S-1). As removal of RB and RG needed to be optimized simultaneously, and to obtain one quadratic model, multiplication of removal efficiency (MRE) of two compounds was applied to achieve a compromise among the responses of the two considered analytes. The main factors, their symbols, levels and design matrix are shown in Table S-1 as well as the response of each run. The variation range of [SDS]/[MIONP] is in the MHAM region. According to the experimental data, a quadratic polynomial model, consists of main effects ([SDS]/ [MIONP] ratio, X_1, and amount of MIONPs, X_2), quadratic effects (X_1^2 and X_2^2), and interaction effects (X_1X_2) was generated (equation (12)):

$$MRE = 0.9331 - 0.0989X_1 + 0.0731X_2 - 0.0632X_1^2 - 0.0409X_2^2 + 0.0613X_1X_2 \quad (12)$$

The obtained data were evaluated by analysis of variance (ANOVA) using STATISTICA 7.0 (Table S-2). The ANOVA table (Table S-2) indicated that the model, main effects, quadratic effects and interaction effects were significant, "Lack of Fit (LOF) p-value" of 0.082121 implies the LOF is not significantly associated to the pure error; furthermore, coefficient of determination, R^2, was 0.98706 which means that the obtained model can explain the variability in response, MRE, very well.[44]

To visualize the relationship between the response and experimental levels of factors, the MRE was mapped against different combinations of two experimental factors in three-dimensional response surface plot (Figure 2). According to the plotted surface, the recovery reached to maximum when the [SDS]/ [MIONP] ratio (X_1) and MIONPs amount (X_2) were around the center point. Finally, the optimum values of [SDS]/ [MIONP] ratio (2.9) and MIONP amounts (87.15 mg) for removal of RB and RG was obtained using a grid search program which had been written in Microsoft Office Excel 2010.

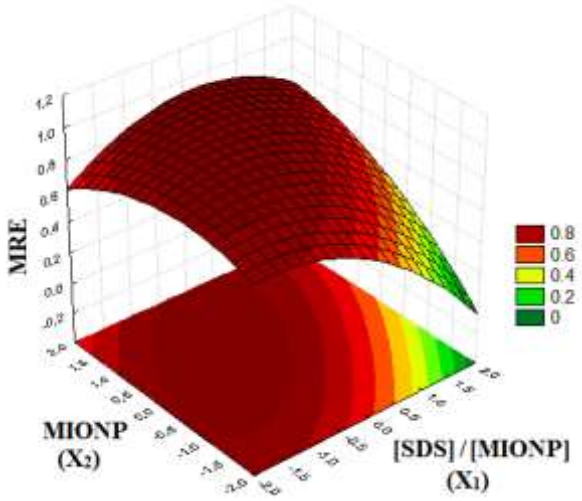

Figure 2. Response surface of the model for simultaneous optimization of [SDS]/[MIONP] ratio (X_1) and amount of MIONPs (X_2).

To evaluate the optimum condition and its predicted response, 5 replications of the experiments under the predicted optimal conditions were performed and for both of the dyes removal efficiency of ~100% were obtained. The relative error in prediction of the removal efficiency was lower than 2.0 %. The weight of damped MHAMS-MIONP adsorbent, provided through the optimum condition, was 4.447 g, while it was 0.143 g for dried adsorbent (about 31 fold less than damped one).

FT-IR spectroscopy. The efficient adsorption of RB and RG was monitored by FT-IR spectroscopy. The FT-IR of RB, RG, MHAMS-MIONPs, and the adsorbed rhodamine dyes on the surface of MHAMS-MIONPs were shown in Figure S-5. The obtained results confirmed the adsorption of RB and RG on the surface of MHAMS-MIONPs.

Study of adsorption kinetic. Study of kinetic of adsorption is important, because this study is not only helpful for the prediction of the adsorption rate and equilibrium time, but also gives important information for designing and modeling of the adsorption processes. Figures S-6(a) and S-6(b) show the removal efficiency versus the contact time. The adsorption rate was too fast so that the equilibrium state obtained only in 4.0 min; which is attributed to the large surface area of MHAMS-MIONPs and its two interaction kinds, i.e. columbic and hydrophobic, with cationic form of RB and RG. Analyzing the kinetic data by pseudo-first order, pseudo-second order, and intra-particle diffusion models (Figures S-6(c) – S-6(h)) indicated that the R^2 values for pseudo-first order and intra-particle diffusion kinetic models were <0.9 and <0.6, respectively. The adsorption data of both of the dyes represented the best fit (R^2 = 1) with pseudo-second-order kinetic model (Figures S-6(e) and S-6(f)). The obtained value of amount of dye adsorbed at equilibrium, q_e (mg g^{-1}), for both RB and RG was 17.51 mg g^{-1}.

Study of adsorption isotherms. Adsorption isotherm equations express the relation between the dye concentrations in solid phase (the mass of the dye adsorbed at constant temperature per unit mass of the adsorbent) and in liquid phase. The experimental data obtained were fitted to the three different adsorption isotherm models including, Langmuir, Freundlich, and Tempkin models (Table 1). While the Langmuir adsorption isotherm assumes mono-layer adsorption of adsorbate onto a homogeneous surface of adsorbent with a finite number of identical sites, the Freundlich model assumes a heterogeneous adsorption of adsorbate onto the surface of adsorbent. Fitting the data in the Langmuir model led to the maximum monolayer capacity, q_{max} (mg g^{-1}), equal to 385 and 323 mg g^{-1}, for RB and RG, respectively; also, fitting the data to the Freundlich model depicted the heterogeneity factors of 3.26 and 3.19. The Tempkin model assumes that heat of adsorption of all molecules in the layer will decrease linearly rather than logarithmic with coverage. The experimental data were fairly well fitted by the Tempkin model; however, the correlation coefficients (tabulated in Table 1) confirmed that the Langmuir model gives better fitting than that of the other models.

Desorption and regeneration studies. Desorption of dyes from MHAMS-MIONPs was tested using different kinds of organic solvents (Figure S-7). The tests were performed by 6 mL of each organic solvent and in three steps (2 mL per step).

The results depicted that a solution of acetic acid in acetonitrile (3% v/v) was found to be an effective elution solvent with desorption efficiency of 96% and 98% for RB and RG, respectively, which shows that the adsorption process is reversible.

The ability of reusing the MIONPs for removal, in several consecutive adsorption and desorption processes, was tested. After each removal, MIONPs were washed by 5 mL acetonitrile (without acetic acid), then by 5 mL water with pH 5, and after that 0.25 g SDS was added to the MIONPs prior to the next adsorption-desorption cycle. The results showed that, after 23 cycles, the depression of MRE was only 5%.

Table 1. Constants and coefficients of various applied isotherms.

Adsorption isotherms	Parameters[a]	Obtained values	
		RB	RG
Langmuir	q_{max} (mg g^{-1})	385	323
	K_L (L mg^{-1})	0.18	-0.25
	R^2	0.9978	0.9963
Freundlich	K_F (L g^{-1})	68.39	57.72
	n	3.26	3.19
	R^2	0.9129	0.8743
Tempkin	A_T (L g^{-1})	15.55	10.18
	RT/b_T	42.94	40.84
	R^2	0.9678	0.9120

Application of MHAMS-MIONPs for the analysis of trace amounts of RB and RG. To apply MHAMS-MIONPs for the trace analysis of RB and RG in real samples, the parameters affecting on the ERs% including volume of elution solvent (3% acetic acid in acetonitrile) and amount of sorbent, MHAMS-MIONPs, were optimized, simultaneously, by CCD. Totally, 16 experiments were performed by 0.5 mg L^{-1} aqueous standard solutions of RG and RB in 50 mL (Table S-3). As the solution of rhodamine dyes in acetonitrile didn't show a good chromatographic behavior, and in order to preconcentrate the anlytes, solvent was evaporated to dryness under a gentle stream of nitrogen; then the residue was dissolved in 150 µL water. Obtaining one quadratic model (equation (13)) for simultaneous optimization of the ERs of RB and RG, multiplication of ERs (MER) was used (Table S-3). The ANOVA table (Table S-4) obtained by the recent experiments, shows that R^2 value is so satisfying (R^2 = 0.98215). Also, by the help of p-values at 95% confidence level, it is obvious that the model, main effects, quadratic effects and interaction effects are significant, while the LOF of the model is not significant.

$$MER = 0.9515 + 0.0751X'_1 + 0.1232X'_2 - 0.0469X'^2_1 - 0.0878X'^2_2 - 0.0232X'_1X'_2 \quad (13)$$

The visualization of the response (MER) versus different combinations of factors experimental levels (Figure 3), together with the grid search procedure indicates that response reaches to maximum when the amount of adsorbent is around the level of 0.6; furthermore, the increase in the elution solvent volume is welcomed, however the enhancement of this factor more than the level 0.6 doesn't change the recovery of the extraction significantly. Finally, 2.6 mL of extraction solvent volume and 90 mg of the amount of adsorbent, i.e. MHAMS-MIONPs, were determined as the optimum conditions, using the grid search method.

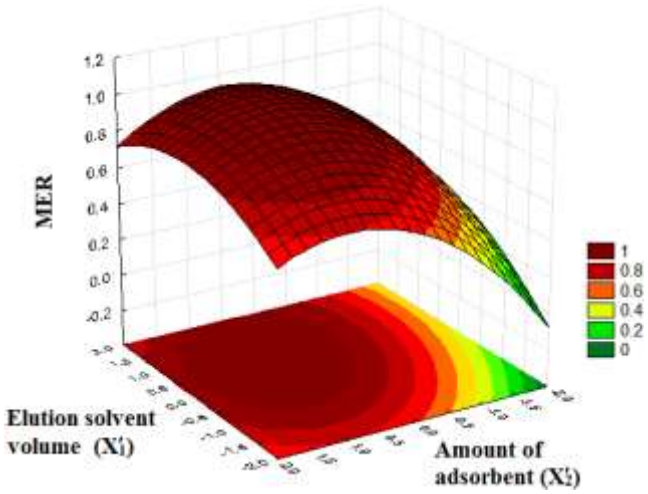

Figure 3. Response surface of the model for simultaneous optimization of volume of elution solvent (X'_1) and amount of MHAMS-MIONPs (X'_2).

Figure of merits of the proposed extraction method and comparison with previous works. The analytical features such as extraction recoveries (ERs), preconcentration factors (PFs), relative standard deviations (RSDs), linear ranges (LRs), determination coefficient (R^2), limits of detection (LODs), and limits of quantification (LOQs) for determination of RB and RG were considered. The ERs% for 0.5 mg L^{-1} of RB and RG standard solutions were 98% and 99%, and PFs were 327 and 330, respectively.

RSD values for five replications of extraction were lower than 4.5%. The linearity was observed over the range of 0.001 – 0.2 mg L^{-1} in the initial solution for both of them, with determination coefficients of 0.9991 for RB and 0.9978 for RG. While the limit of detection and quantification, defined as LOD = $3S_b/m$ and LOQ = $10S_b/m$ (where S_b is the standard deviation of blank and m is the slope of calibration graph after preconcentration), for RB were 0.34 and 1.12 ng mL^{-1} (n = 10), they were 0.21 and 0.69 ng mL^{-1} (n = 10) for RG, respectively.

Only few methods are available for simultaneous determination of RB and RG.[19, 20, 22] Table 2 shows the other methods applied for determination of RB and RG, simultaneously. In comparison with previous works the proposed method shows very high preconcentration factor, the better LOD and desirable linear range for quantitative analysis of RB and RG.

Interference of ionic species. The compositions of environmental and waste water samples are usually complex, and

they contain particularly different kinds of ionic species, which may interfere in the extraction and determination process. In order to study on the effect of potentially interfering ions on the extraction of 0.5 mg L-1 standard solution RB and RG, tolerance ratio of the method to the different cations (Na^+, K^+, Mg^{2+}, Ca^{2+}, and Fe^{3+}) and anions (NO_3^-, CO_3^{2-}, and PO_4^{3-}) was examined. In Table S-5, the tolerance ratio shows the ratio of the interfering agent concentration to the concentration of analytes causing a relative error in the MER less than 10%. The results showed that ER of the analytes in the presence of interfering ions at the ratios that usually occur in the real samples is quantifiable using the proposed method.

Application of the proposed method for real samples. To evaluate the applicability of the proposed method in real samples for both removal of RB and RG from the waste waters and for the determination of trace amounts of these dyes, three different water samples, including municipal waste water sample of Antwerp, waste water of the University of Antwerp, and the Schelde river water sample were tested. For the aim of removal, all the samples were spiked with RB and RG standards at three levels in 50 mL solutions; subsequently, they were removed using the MHAMS-MIONPs (under optimum condition: pH of the sample solution = 2; amount of MIONPs = 87.15 mg; [SDS]/[MIONP] ratio = 2.9). Also, for the aim of determination, all the samples were spiked with rhodamine dye standards at five levels in 50 mL solutions and extractions were performed under optimum condition: pH of the sample solution = 2; amount of damped MHAMS-MIONPs = 90 mg; eluent solvent volume = 2.6 mL, 3% acetic acid in acetonitrile.

The average results of three repetitive analysis of each sample showed REs% about 100% with RSDs (n=3) less than 0.2 % and the ERs% between 92.25% and 96.38% with RSDs (n=3) less than 5.0 % (Table S-6). This indicates that with respect to the complexity of the matrices studied, the values of ERs% and REs%, obtained by the proposed method, are in satisfactory agreement with the added amounts of dyes standards.

CONCLUSION

In this paper, a special kind of SDS-coated MIONPs, i.e., MHAMS-MIONPs were applied for both removal and determination of RB and RG, as two of the most important xanthine dyes, in waste water and environmental water samples. The zeta potential measurements were used to determine the [SDS]/[MIONP] ratios at which the SDS molecules are able to form mixed hemi/ad-micelle, MHAM, on the surface of MIONPs. The MHAM not only protected the MIONPs chemically and physically, but also this kind of SDS molecular array provided a substrate around the MIONPs which was able to attract positive form of RB and RG electrostatically and to have hydrophobic interaction with them.

The parameters affecting the adsorption of RB and RG were optimized to obtain the best conditions for their removal. Investigations of the pH factor was performed by one variable at-a-time; and because of the significant interaction, the two other significant factors, i.e. amount of MIONPs and [SDS]/[MIONP] ratios, were optimized by response surface methodology through CCD. Under optimum condition, the kinetics of the adsorption was investigated; and obtained results indicated that the pseudo-second-order model provided the best correlation of the adsorption data and the adsorption equilibrium was best defined by the Langmuir isotherm model.

Overall, this paper presents the optimal condition for preparation of MHAMS-MIONPs, as a selective, powerful and efficient adsorbent with the fast adsorption kinetics, good adsorption capacity, excellent reusability as well as the high chemical stability for removal of rhodamine dyes from water samples. Furthermore, utilization of this adsorbent in MNP-SPE showed sufficient specificity, selectivity and sensitivity in determination of RB and RG in trace levels for conducting studies on environmental pollution of water samples and quality control of water treatment plants.

AUTHOR INFORMATION

Corresponding Author

M. R. Hadjmohammadi

(Tel & fax: +981125342350; E-mail address: hadjmr@umz.ac.ir)

ASSOCIATED CONTENT

Supporting Information

The Supporting Information contains discussion on synthesis of MIONPs, instrumentation and operating conditions, figure for characterization of synthesized MIONPs (Figure S-1), characterization of MIONPs and MHAMS-MIONPs by DLS

Table 2. Comparison of the present work with other methods for determination of RG and RB, simultaneously.

Method	Extractant	Dye	LOD [a]	LR [a]	R^2	RSD (%)	PF
SPE-HPLC-FLD [b 20]	Methanol+Formic Acid	RB	0.5×10^{-3}	2-50 50-1000	0.9950 0.9999	3	-
		RG	0.1×10^{-3}	0.5-20 20-400	0.9940 0.9994	3	-
DLLME-Vis[22]	Chloroform	RB RG	0.48-1.93	5-450	0.9958-0.9997	<4.7	20
MSA-DLLME-Vis[19]	1-Octanol	RB	1.23	7.5-1000	0.9999	1.21	48
		RG	1.15	5-1000	0.9999	0.94	46
Present work	3% Acetic Acid in Acetonitrile	RB	0.34	0.001- 0.2	0.9991	4.3	327
		RG	0.21	0.001- 0.2	0.9978	3.9	330

[a] (ng mL^{-1})

[b] Fluorescence detection

and TEM, figure for size distributions of MIONPs (Figure S-2a) and MHAMS-MIONPs (Figure S-2b) by DLS, TEM images of bare MIONPs (Figure S-3a), and MHAMS-MIONPs (Figure S-3a), figure for investigation of the effect of pH of the sample solution on removal efficiency (Figure S-4), description of CCD experiments for simultaneous optimization of [SDS]/ [MIONP] and amount of MIONP, a table which shows the main factors, symbols, levels and design matrix for simultaneous optimization of [SDS]/ [MIONP] ratio and amount of MIONPs by Table S-1 with its ANOVA table (Table S-2), figure for FT-IR spectra of RB, RG, MHAMS-MIONP, and MHAMS-MIONPs-RB/RG (Figure S-5) and its description, figure for adsorption kinetic studies (Figure S-6), a figure which indicates the effect of different kinds of elution solvents on recovery of the dyes (Figure S-7), a table which shows main factors, symbols, levels and design matrix for simultaneous optimization of elution solvent volume and amount of MHAMS-MIONPs (Table S-3) together with ANOVA table (Table S-4), a table for investigation of Interference of ionic species (Table S-5), and a table which represents the removal and determination of RB and RG in waste and environmental water samples (Table S-6). This material is available free of charge via the Internet at http://pubs.acs.org.

REFERENCES

(1) Neckers, D. C.; Valdes-Aguilera O. M. In *Advances in Photochemistry*; Volman, D., Hammond, G. S., Neckers, D. C., Eds.; Wiley: New York 1993; pp 315–370.

(2) Hood, R. D.; Jones, C. L.; Ranganathan, S. *Teratology* **1989**, *40*, 143−150.

(3) Wuebbles, B. J. Y.; Felton, J. S. *Environ. Mutagen.* **1985**, *7*, 511−522.

(4) Sweatman, T. W.; Seshadri, R.; Israel, M. *Cancer Chemother. Pharm.* **1990**, *27*, 205−210.

(5) Thaler, S.; Haritoglou, C.; Choragiewicz, T. J.; Messias, A.; Baryluk, A.; May, C. A.; Rejdak, R.; Fiedorowicz, M.; Zrenner, E.; Schuettauf, F. *Invest. Ophthalmol. Vis. Sci.* **2008**, 49, 2120–2126.

(6) Alesso, M.; Bondioli, G.; Talío, M.C.; Luconi, M.O.; Fernández, L.P. *Food Chem.* **2012**, *134*, 513–517.

(7) Aarthi, T.; Madras G. *Ind. Eng. Chem. Res.* **2007**, *46*, 7–14.

(8) Priya, M. H.; Madras G. *Ind. Eng. Chem. Res.***2006**,*45*, 913–921.

(9) Merouani, S.; Hamdaoui, O.; Saoudi, F.; Chiha, M.; Pe´trier, C. J. Hazard. Mater. **2010**, 175, 593–599.

(10) Selvam, P. P.; Preethi, S.; Basakaralingam, P.; Thinakaran, N.; Sivasamy, A.; Sivanesan, S. J. Hazard. Mater. **2008**, 155, 39–44.

(11) Mohammadi, M.; Hassani, A. J.; Mohamed, A. R.; Najafpour, G. D. J. Chem. Eng. Data 2010, 55, 5777–5785.

(12) Sumanjeet, T. P. S.; Walia, I. K., J. Surf. Sci. Technol. **2008**, 24, 179–193.

(13) Travlou, N. A.; Kyzas, G. Z.; Lazaridis, N. K.; Deliyanni, E. A. *Langmuir* **2013**, *29*, 1657–1668.

(14) Mak, S. Y.; Chen, D. H. *Dyes and Pigments* **2004**, 61, 93–98.

(15) Huang, Y.; Keller, A. A. *ACS Sustainable Chem. Eng.* **2013**, 1, 731–736.

(16) Biparva, P.; Ranjbari, E.; Hadjmohammadi, M. R. *Anal. Chim. Acta* **2010**, 674, 206–210.

(17) Pourreza, N.; Rastegarzadeh, S.; Larki, A. *Talanta* **2008**, 77, 733–736.

(18) Ren, H.; Kulkarni, D. D.; Kodiyath, R.; Xu, W.; Choi, I.; Tsukruk, V. V. *ACS Appl. Mater. Interfaces* **2014**, *6*, 2459–2470.

(19) Ranjbari, E.; Hadjmohammadi, M. R. *Talanta* **2015**, *139*, 216–225.

(20) Chiang, T. L.; Wang, Y. C.; Ding, W. H. *J. Chin. Chem. Soc-Taip.* **2012**, *59*, 515–519.

(21) Lu, Q.; Gao, W.; Du, J.; Zhou, L.; Lian, Y. *J. Agr. Food Chem.* **2012**, *60*, 4773–4778.

(22) Xiao, N.; Deng, J.; Huang, K.; Ju, S.; Hu, C.; Liang, J. *Spectrochim. Acta A* **2014**, *128*, 312–318.

(23) Anirudhan, T. S.; Rejeena, S. R.; Binusree, J. *J. Chem. Eng. Data* **2013**, *58*, 1329–1339.

(24) Shen, L.; Laibinis, P. E.; Hatton, T. A. *Langmuir* **1999**, *15*, 447–453.

(25) Harris, L. A.; Goff, J. D.; Carmichael, A. Y.; Riffle, J. S.; Harburn, J. J.; St. Pierre, T. G.; Saunders, M. *Chem. Mater.* **2003**, *15*, 1367–1377.

(26) Chen, C. T.; Chen, Y. C. *Anal. Chem.* **2005**, *77*, 5912–5919.

(27) Lo, C. Y.; Chen, W. Y.; Chen, C. T.; Chen, Y. C. *J. Proteome Res.* **2007**, *6*, 887–893.

(28) Chen, C.-T.; Chen, W. Y.; Tsai, P. J.; Chien, K. Y.; Yu, J. S.; Chen, Y. C. *J. Proteome Res.* **2006**, *6*, 316–325.

(29) Iida, H.; Takayanagi, K.; Nakanishi, T.; Osaka, T. *J. Colloid Interf. Sci.* **2007**, *314*, 274–280.

(30) Zhao, X.; Li, J.; Shi, Y.; Cai, Y.; Mou, S.; Jiang, G. *J. Chromatogr. A* **2007**, *1154*, 52-59.

(31) Liu, Q.; Shi, J.; Wang, T.; Guo, F.; Liu, L.; Jiang, G. *J. Chromatogr. A* **2012**, *1257*, 1-8.

(32) Huang, C.; Hu, B. *Spectrochim. Acta Part B* **2008**, *63*, 437-444.

(33) Faraji, M.; Yamini, Y.; Rezaee, M. *J. Iran. Chem. Soc.* **2010**, *7*, 1-37.

(34) Shen, H. Y.; Zhu, Y.; Wen, X. E.; Zhuang, Y. M. *Anal. Bioanal. Chem.* **2007**, *387*, 2227-2237.

(35) Banerjee, S. S.; Chen, D. H. *J. Hazard. Mater*. **2007**, *147*, 792-799.
(36) Zhao, X.; Shi, Y.; Wang, T.; Cai, Y.; Jiang, G. *J. Chromatogr. A* **2008**, *1188*, 140-147.
(37) Ho, Y. S.; McKay, G. *Water Res.* **1999**, *33*, 578-584.
(38) Ho, Y. S.; McKay, G.; Wase, D. A. J.; Forster, C. F. *Adsorpt. Sci. Technol.* **2000**, *18*, 639-650.
(39) Weber, W. J.; Morris, J. C. *J. Sanit. Eng. Div. Am. Soc. Civ. Eng.* **1963**, *89*, 31-60.
(40) Langmuir, I. *J. Am. Chem. Soc.* **1918**, *40*, 1361-1403.
(41) Freundlich, H. M. F. *J. Phys. Chem.* **1906**, *57*, 385–470.
(42) Temkin, M. I.; Pyzhev, V. *U.R.S.S.* **1940**, *12*, 217-222.
(43) *Drug Bank* Website; http://www.drugbank.ca/drugs/DB03825.
(44) Mchedlov-Petrossyan, N. O.; Kukhtik, V. I.; Alekseeva, V. I. *Dyes Pigments* **1994**, *24*, 11-35.
(45) Morgan, E. D. *Chemometrics: experimental design*, Wiley: New York, 1995.

For TOC only

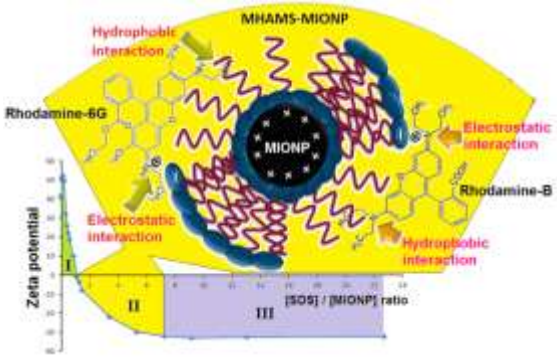
MHAMS-MIONP
Hydrophobic interaction
Rhodamine-6G
MIONP
Electrostatic interaction
Rhodamine-B
Electrostatic interaction
Hydrophobic interaction
Zeta potential
I
II
III
[SOS] / [MIONP] ratio